Dynamic Response of BLDC-Thruster for Small Scale Quadrotors under Aerodynamic Load Torque

Conference Paper · November 2014

DOI: 10.1109/ROPEC.2014.7036341

CITATIONS
8

READS
1,558

4 authors:

Ricardo Martinez Alvarado
Instituto Tecnológico Nacional de México - Instituto Tecnológico de Saltillo
6 PUBLICATIONS **23** CITATIONS
SEE PROFILE

Francisco José Ruiz-Sánchez
CINVESTAV - Saltillo
54 PUBLICATIONS **183** CITATIONS
SEE PROFILE

Anand Sanchez-Orta
Center for Research and Advanced Studies of the National Polytechnic Institute
112 PUBLICATIONS **1,478** CITATIONS
SEE PROFILE

Octavio Garcia Salazar
Autonomous University of Nuevo León
82 PUBLICATIONS **663** CITATIONS
SEE PROFILE

Dynamic Response of BLDC-Thruster for Small Scale Quadrotors under Aerodynamic Load Torque

Ricardo Martinez-Alvarado, Francisco J. Ruiz-Sanchez, Anand Sanchez-Orta
Robotica y Manufactura Avanzada
CINVESTAV-Saltillo
A.P. 663
25000 Saltillo, Coah.
Mexico
Email: ricardo.martinez@cinvestav.edu.mx, {fruiz, anand.sanchez}@cinvestav.mx

Octavio Garcia-Salazar
CIIIA-FIME
Av. Universidad s/n
Universidad Autonoma de Nuevo Leon
66452 San Nicolas de los Garza, N.L.
Mexico
Email: octavio.garcia@uanl.mx

***Abstract*—In multi-rotor UAVs, a controlled Thrust is a main factor to achieve a safe and stable flight. Thrust is the result of a coordinated action of a set of symmetrically distributed thrusters whose single contribution is usually described as a square function of its rotor speed; however, aerodynamic forces induce a load torque on the rotor that disturb its expected speed response, thus its effective Thrust, affecting the whole performance of the aircraft. In this paper, we analyse and quantify the effects of the aerodynamic load torque induced on the spinning propeller of a BLDC thruster used in small scale Quadrotors and present some experimental validation. We describe the model of a 3-phase thruster with a two blade propeller of fixed pitch angle, we analyse its numerical simulation to determine the effects of the induced load torque on the dynamic response of the rotor, and we experimentally verify the results assuming ideal conditions of hover flight. Finally we illustrate the convenience of using feedback control to reduce the sensibility of thrusters face to non modelled dynamics applying a PD controller and we discuss about the importance of an accurate dynamic model of the thruster for control purposes.**

I. Introduction

Unmanned Aerial Vehicles (UAVs), or drons, are flying vehicles without pilot on board, teleoperated and provided with a certain degree of autonomy. Their potential in civilian and military applications, specially in dangerous or inaccessible environments for humans, has already caught the attention of engineers and their development has become a research area in its own right because of the basic and applied research problems it poses. Among their configurations, Quadrotor, a multi-rotor rotary wing aircraft, receives special attention thanks to its simple architecture, small size, great flexibility, and safety for indoor and outdoor flight.

Quadrotors have four, coplanar and parallel, thrusters arranged symmetrically in a diamond configuration around a main axis, with two sets of opposite and counter-rotating rotor pairs. Their flight is controlled varying the Thrust of the rotor pairs, for instance, total Thrust for altitude, momenta of the differential Thrust between opposite rotors for pitch and roll, and difference in reaction torques between the pitch and roll rotor pairs for yaw [1]. In miniature models, thrusters are Brush Less DC motors (BLDC motors) with fixed blade pitch angle propellers, whose Thrust has been theoretically described as a square function of its rotor speed with constant parameters determined by geometrical properties of the propeller [2], [3], and their speed is regulated using a DC input of reference, electronically commutated to an AC signal.

Commercial thrusters, BLDC motor and electronic driver, are for users, black box systems with unknown inner control loops and start-up strategies, presumed to offer an ideal dynamic response compensating uncertainties, for instance, non modelled dynamics of power supply [5] or aerodynamic load torque induced by the turning propeller [6]. However, their performance, under identical, configurations and experimental conditions, is not the same. These variations introduce additional uncertainties to the whole dynamics of the Quadrotor, assumed to be compensated during the flight by a master controller, but in fact, increasing the demand of control and the risk of instability; impacting on its energy consumption.

Nowadays, Quadrotors are required to realize long duration and high demanding tasks, as collaborative and aggressive manoeuvres in non-structured environments, and they must be provided with better controllers to face the variant an unpredictable conditions of flight. A better understanding of their dynamics, starting with a more realistic model of the thrusters, could be very useful when modern control approaches are used to improve their performance during the flight. The free dynamics of a BLDC motor, described as a two-pole system [4], has been improved in [5], introducing one zero due to the dynamics of the battery, and it has been showed how this model can be used to enhance the performance of the thruster decreasing its rise-time and increasing the disturbance rejection with a proportional controller. However, this model neglect electric and aerodynamic dynamics which become important as the thruster is required to have fast reactions as in the quadrotors. In [3] aerodynamic load torque is introduced as quadratic function of the angular velocity but this expression does not allow a better understanding of designing factors for control purposes. In nautical application, it has been showed that introducing the dynamics of the load torque produced by the spinning propeller into the dynamic model of the thruster can be used to improve its performance during speed changes, particularly when starting or during speed-up time ([7], [8]). In this paper, we improve the dynamical description of thrusters for control purposes started in [6], we analyse the total load torque induced on a BLDC motor by aerodynamic forces on the spinning propeller, we obtain the BLDC/propeller and we simulate its dynamical behaviour under hover conditions to

show the effects of the aerodynamic forces, fist, on the total load torque and, then, on the increment of current consumption when the rotor is required to maintain a constant speed. We validated these results experimentally and additionally we illustrate the potential of the composed model for control purposes showing the improved performance obtained with a PD controller.

II. Dynamic Model of the BLDC/Propeller System

Thrusters for miniature quadrotors are 3-phase BLDC motors with fixed blade pitch angle propellers because of its efficiency and low torque ripple. They can be modelled straightforward as a coupled model BLDC/propeller introducing the aerodynamic effects of the turning propeller to the electric and mechanical dynamics of rotor.

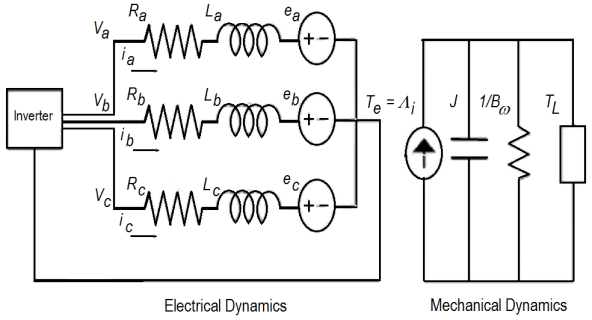

Fig. 1: Model of the BLDC motor where mechanical dynamics is described using the current-torque analogy.

A. Model of the 3-phase BLDC Motor

A 3-phase BLDC motor is a synchronous machine with a permanent magnet rotor and windings pairs symmetrically distributed in the stator (every $120°$) which are pairs activated by a PWM inverter, i. e. energizing two phases simultaneously with a switching frequency determined by the position and speed of the rotor [9]. According to [10] and [14], if the three phases are assumed to be balanced and, saturation, Eddy currents and hysteresis are neglected, it can be described as an hybrid model (showed in Fig. 1) by the equations

$$\begin{aligned} V_{ab} &= R(i_a - i_b) + L\tfrac{d}{dt}(i_a - i_b) + e_a - e_b, \\ V_{bc} &= R(i_b - i_c) + L\tfrac{d}{dt}(i_b - i_c) + e_b - e_c, \\ V_{ca} &= R(i_c - i_a) + L\tfrac{d}{dt}(i_c - i_a) + e_c - e_a, \\ T_e &= J\tfrac{d\omega_m}{dt} + B_m\omega_m + T_L, \end{aligned} \tag{1}$$

where V, i, and e are, respectively, voltage, current and induced voltage (back emf) between phases ab, ac or bc; R and L, the resistance and inductance, assumed the same in all phases, T_e, the electrical torque, J, the inertia, ω_m, the angular speed, B_m, the viscous friction coefficient, and T_L, the load torque. The induced voltage can be expressed as $e_a = k_e\omega_m F(\theta_e)$, $e_b = k_e\omega_m F(\theta_e - \frac{2\pi}{3})$, $e_c = k_e\omega_w F(\theta_e - \frac{4\pi}{3})$ and the electric torque

$$T_e = \frac{k_t}{2}[F(\theta_e)i_a + F(\theta_e - \frac{2\pi}{3})i_b + F(\theta_e - \frac{4\pi}{3})i_c],$$

with k_e and k_t, constants of the induced voltage and torque, respectively, θ_e, the electric angle (equal to the rotor angle), θ_m (expressed in rad) times the number of pole pairs, $\theta_e = \frac{p}{2}\theta_m$, and the function $F(\cdot)$, a carrier signal that represents the trapezoidal waveforms of the induced voltage

$$F(\theta_e) = \begin{cases} 1 & 0 \le \theta_e < \frac{2\pi}{3} \\ 1 - \frac{6}{\pi}(\theta_e - \frac{2\pi}{3}) & \frac{2\pi}{3} \le \theta_e < \pi \\ -1 & \pi \le \theta_e < \frac{5\pi}{3} \\ -1 + \frac{6}{\pi}(\theta_e - \frac{5\pi}{3}) & \frac{5\pi}{3} \le \theta_e < 2\pi \end{cases}. \tag{2}$$

Equation (1) can be written in the form of state variables,

$$\begin{aligned} \dot{x} &= Ax + Bu + \eta, \\ y &= Cx, \end{aligned} \tag{3}$$

with

$$x = \begin{pmatrix} i_a \\ i_b \\ \omega_m \\ \theta_m \end{pmatrix}, u = \begin{pmatrix} V_{ab} - e_{ab} \\ V_{bc} - e_{bc} \\ T_e \end{pmatrix}, y = \begin{pmatrix} i_a \\ i_b \\ i_c \\ \omega_m \\ \theta_m \end{pmatrix}, \eta = \begin{pmatrix} 0 \\ 0 \\ -\frac{T_L}{J} \\ 0 \end{pmatrix},$$

and $e_{ab} = e_a - e_b$, $e_{bc} = e_b - e_c$,

$$A := \begin{pmatrix} -\frac{R}{L} & 0 & 0 & 0 \\ 0 & -\frac{R}{L} & 0 & 0 \\ 0 & 0 & -\frac{B_m}{J} & 0 \\ 0 & 0 & 1 & 0 \end{pmatrix}, B := \begin{pmatrix} \frac{2}{3L} & \frac{1}{3L} & 0 \\ -\frac{1}{3L} & \frac{1}{3L} & 0 \\ 0 & 0 & \frac{1}{J} \\ 0 & 0 & 0 \end{pmatrix},$$

$$C = \begin{pmatrix} 1 & 0 & 0 & 0 \\ 0 & 1 & 0 & 0 \\ -1 & -1 & 0 & 0 \\ 0 & 0 & 1 & 0 \\ 0 & 0 & 0 & 1 \end{pmatrix}$$

where the input η is the load torque induced by aerodynamic forces acting on the propeller.

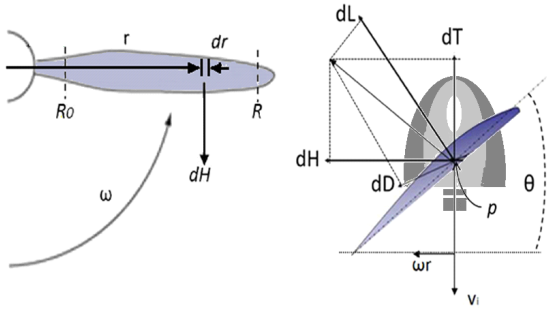

Fig. 2: Aerodynamic forces on the propeller described by the Blade Element Approach.

B. Aerodynamic Forces on a Propeller with a Fixed Pitch Blade Angle

Aerodynamic forces acting on a spinning propeller can be calculated based on the Blade Element Theory [11]. From Figure 2, the differential expressions of Thrust, dT, and Drag,

dH, in terms of the induced velocity, v_i, and the rotor speed, ω_r, are

$$\begin{array}{rl} dT = & \frac{1}{2}\rho c(r) C_L(\alpha(\theta, v_i)) u^2 dr \\ dH = & \frac{1}{2}\rho c(r) C_D(\alpha(\theta, v_i)) u^2 dr \end{array} \quad (4)$$

with $\alpha(\theta, v_i))$, $c(r)$ and $\theta(r)$, the angle of attack, the chord and the pitch, and C_L, C_D, the coefficients of lift and drag, respectively, where $u^2 = v_i^2 + \omega^2 r^2$ and from experimental data $C_L = l_0 + l_1\alpha(\theta, v_i)$ and $C_D = d_0 + d_1\alpha(\theta, v_i) + d_2\alpha^2(\theta, v_i)$. Assuming a propeller with a small symmetrical blade such that $c(r) = c$, $\theta(r) = \theta$, $\alpha(v_i) = \theta - arctan(\frac{v_i}{\omega r})$; recalling that $dT_L = rdH$, and integrating along the radius of the blade, from R_0 to R_h, Thrust, T, and Load Torque, T_L, can be expressed as

$$\begin{array}{rl} T = & \frac{1}{2}\rho c \Bigg\{ \frac{1}{3}\frac{l\,\theta\left(v_i^2+\omega^2 r^2\right)^{\frac{3}{2}}}{\omega} - \frac{l\, v_i \omega\, r^2}{2} \\ & -\frac{1}{2}\left[r\sqrt{v_i^2+\omega^2 r^2} + \frac{v_i^2 \ln\left(\omega r + \sqrt{v_i^2+\omega^2 r^2}\right)}{\omega} \right] \\ & \left(d_0 + d_2\theta^2\right) v_i + 2 d_2 \theta v_i^2 r \\ & -\frac{d_2 v_i^3 \ln\left(\omega\, r + \sqrt{v_i^2+\omega^2 r^2}\right)}{\omega} \Bigg\}_{R_0}^{R_h}, \end{array}$$

$$\begin{array}{rl} T_L = & \frac{1}{2}\rho c \Bigg\{ \frac{1}{3}\frac{(v_i^2+\omega^2 r^2)^{3/2} l\theta v_i}{\omega^2} - \frac{1}{2} r^2 l\theta v_i^2 \\ & +\frac{1}{4}\frac{d_0 r (v_i^2+\omega^2 r^2)^{\frac{3}{2}}}{\omega} - \frac{1}{8}\frac{d_0 v_i^2 r\sqrt{v_i^2+\omega^2 r^2}}{\omega} \\ & -\frac{1}{8}\frac{d_0 v_i^4 \ln\left(\omega r + \sqrt{v_i^2+\omega^2 r^2}\right)}{\omega^2} \\ & +\frac{1}{3} d_2 \theta^2 \omega r^3 - \frac{2}{3} d_2 \theta v_i \omega r^3 \\ & +\frac{1}{2}\frac{d_2 v_i^2 r\sqrt{v_i^2+\omega^2 r^2}}{\omega} \\ & -\frac{1}{2}\frac{d_2 v_i^4 \ln\left(\omega r + \sqrt{v_i^2+\omega^2 r^2}\right)}{\omega^2} \Bigg\}_{R_0}^{R}. \end{array} \quad (5)$$

On the other hand, induced velocity, v_i, under hover conditions, can be expressed as a function of Thrust using the conservation of momentum [11] [12] [13], i.e.,

$$v_i = \sqrt{\frac{T}{2\,\rho\, A_d}} \quad (6)$$

with $A_d = \pi R_h^2$ the section area of the turning propeller and ρ the density of the air (Figure 3).

C. BLDC/Propeller Model

The dynamic model of the coupled BLDC/Propeller system results from defining $\omega_m := \omega$ in equations (3) and (5), and coupling the Load Torque in both models as showed in the block diagram of Figure 3.

This composed model introduces a closer description of the dynamic of the load torque produced by aerodynamic forces than the quadratic function of the angular velocity, $T_L = k_f\omega^2$, with k_f a constant, presented in [3].

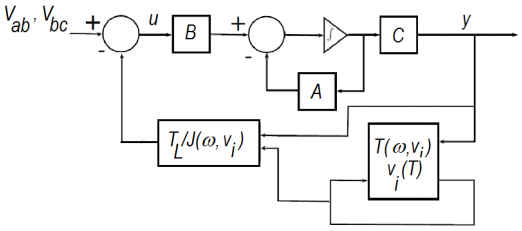

Fig. 3: Block diagram of the BLDC/Propeller system

III. Simulation Analysis of the BLDC/Propeller System

In order to analyse and quantify the effects of the aerodynamic load torque, T_L, on the thruster dynamics, we simulated the BLDC/Propeller model of Equations (3) and (5) with parameters of the real BLDC motor implemented in our experimental platform [15], showed in Table I, using MATLAB R2009b.

TABLE I: Parameters of the BLDC/Propeller system

Parameter	Value	Units
R	$0.30/2$	Ohm
L	$0.080 \times 10^{-3}/2$	H
V_s	12	V
k_t	20×10^{-3}	Nm/A
k_e	20×10^{-3}	$Volts/(rad/sec)$
P	2	pu
J	119×10^{-7}	kgm^2
B_m	0	Nm/s
ρ	1.124	kg/m^3
r	$R - R_0$	m
R	14.5×10^{-2}	m
R_0	2.5×10^{-2}	m
A_d	πr^2	m^2
c	1.7×10^{-2}	m
θ	6	deg
l	$0.57296/2$	pu
d_0	$0.000594/2$	pu
d_2	$0.01778/2$	pu

A. Simulation of the BLDC Motor

First, we simulated the model of the BLDC motor (Eq.(3)) reaching freely a constant speed and then perturbed with a constant load torque. In this way, we simultaneously verified the accuracy of the BLDC model with respect to the manufacturer's specification, and we obtained a pattern of the motor dynamics that can be useful to determine the effects of the aerodynamic load torque introduced by the turning propeller. At 5700 rpm constrained to a load torque of 180 Nm; the current and the electric torque match the nominal values with an error of less than 5%. We illustrate the results obtained in Figure 4 where we present the phases of the BLDC motor, the electric torque, current consumption, rotor speed, and the Electric Torque vs Rotor Speed. After the rotor attain a constant speed, the energy consumption stops (observe the current of the three phases) and when the constant load torque is applied, the energy consumption restarts introducing residual oscillations. This is because of the assumption of a negligible friction, $B_m = 0$, (see Table I and Eq.(1)), requiring no forces,

therefore, none energy, to reach a steady state unless a load torque is applied.

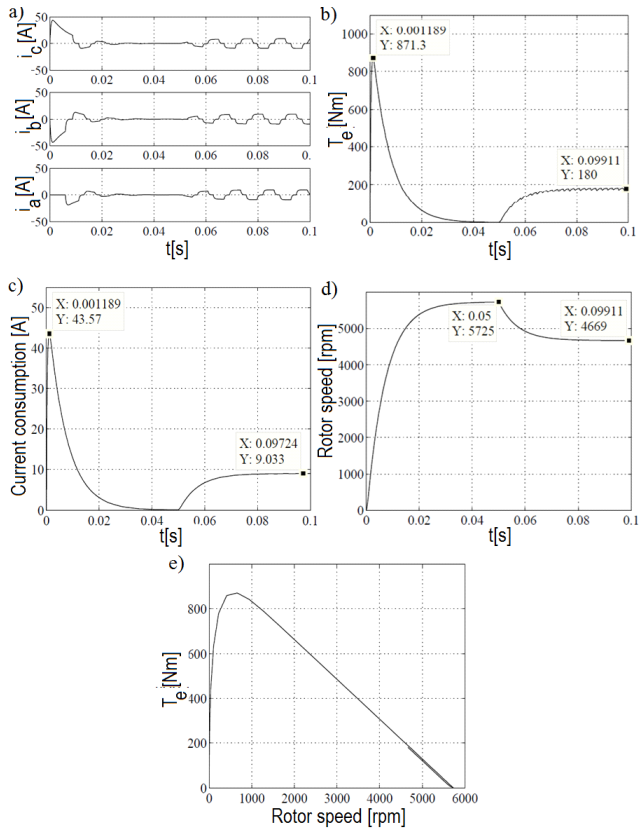

Fig. 4: BLDC Model: desired rotor speed $\omega_m = 5700rpm$, constant Load Torque, $T_L = 180Nm$, at $t = 0.05s$. Phase currents (a), Electric Torque (b), Current consumption (c), Rotor Speed (d), Electric Torque vs Rotor Speed (e).

B. Simulation of the BLDC/Propeller Model

Afterwards, we simulated the BLDC/Propeller model (Figure 3) under the same conditions as in the previous case without the perturbing load torque. Results, with a desired rotor speed of $5700rpm$, are showed in Figure 5. The final rotor speed is lower than the desired one, as in the case of the free model facing a constant load torque, but in this case, the continuous action of the aerodynamic load torque on the rotor slows down the whole response and increases the current consumption (steady state oscillations), either while reaching the desired Thrust or when the BLDC motor is holding it; thus the load torque introduced by the spinning propeller modifies the general dynamics of the system, with a delay in the response and a steady state error which increases as the desired speed of the rotor increases, affecting the performance of the thruster specially under fast reactions. Observe that load torque, T_L, described by Equation (5), is not only an opposite force depending on the rotor speed, as in [3], but an expression that allows a better understanding of some designing factors of a thruster, as the angle of attack and the size of the propeller, related to the induced velocity and the coefficients of Lift and Drag. For example, if the angle of attack in the propeller, θ, is increased from $6°$ to $16°$, the load torque is such that the final

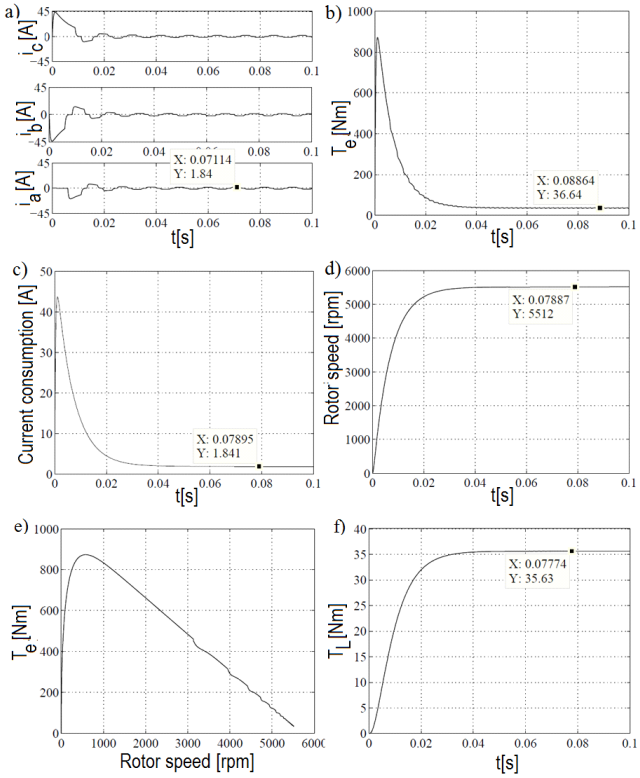

Fig. 5: BLDC/Propeller Model: desired rotor speed $\omega_m = 5700rpm$. Phase currents (a), Electric Torque (b), Current consumption (c), Rotor Speed (d), Electric Torque vs Rotor Speed (e).

speed, is about 10% under the desired value, that is, instead of $5700rpm$, it is $5060rpm$.

IV. Experimental Analysis

We verified the accuracy of the BLDC/propeller model by means of experimental results obtained with a standard thruster (BLDC motor, driver and propeller) used in quadrotors (see TableII). The control input uses a Pulse Position Modulation with a pulse width from $1ms$ to $2ms$.

TABLE II: Technical data of the Thruster

Device	Description
BLDC motor	Booster Engine 10/1200, Booster EngineOhm
Power Supply	Lythium Ploymer, 3s, 11.1V, 2.1A, 23.5Wh, E-flite
Driver	EFLA 325H, 25 A, Helicopter Brushless ESC, E-flite
Propeller	10X4.5 anti clockwise, MAXX products

A. Experimental Setup

The experimental set-up is a mechanical device in see-saw configuration designed to measure the lifting force produced by the thruster in a resistive sensor (Figure 6). It is provided with a data acquisition system for measuring force, rotor speed and current consumption, based on a data acquisition board (National Instruments, PCI-6024E) with a sampling time up

to 200 kHz, and xPC Target library of MATLAB/Simulink. Experimental conditions are based on the numerical simulation

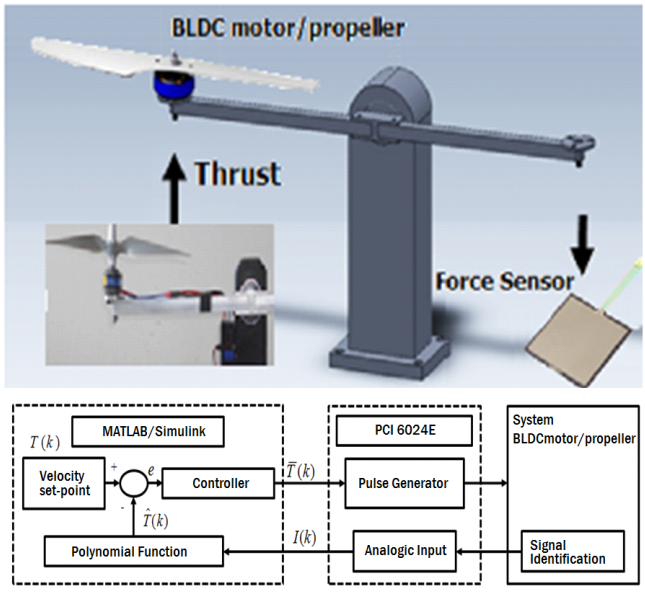

Fig. 6: Experimental setup

using the same step response in order to compare the dynamic behaviour of the real thruster and the simulated one, and then, to evaluate the accuracy of the model. Data, were filtered digitally by a Butterworth filter with a bandwidth of 3Hz to help their analysis eliminating noise produced by parasite vibrations as showed in Figure 7.

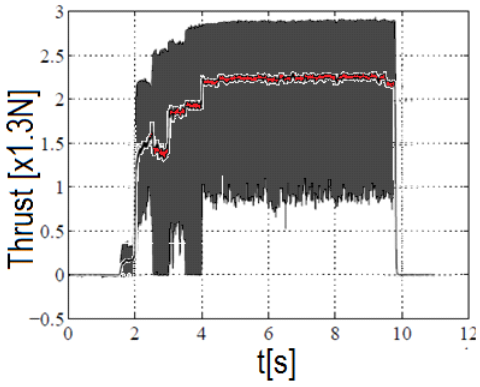

Fig. 7: Example of Experimental and Filtered Data.

B. Step Response of the BLDC/Propeller System

We tested the step response of the thruster in different operation regimes of the attainable rotor speed, determined by the permissible input pulse width. We observed that in a low speed regime, simulation and experimental results are qualitatively similar. Even, if the dynamic of the real system is slower than the calculated in simulations, rotor-speed and force follow the step input very close, with a reduction on the input-output rate produced by the aerodynamic forces increasing the load torque. This could be explained by the assumptions neglecting frictions and inertias (Fig.8). However, in high speed regime, the response presents an important overshoot, a long settling time with an important reduction of the input-output rate, and an increment on the current consumption (Fig.9). We presume that this behaviour is not only due to physical factors but to the dynamics introduced by the internal design of the commercial driver.

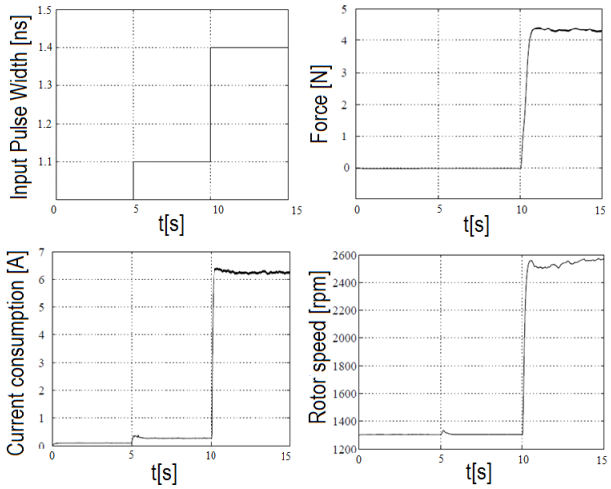

Fig. 8: Step response of the BLDC Thruster: low rotor speed regime(max pulse width 1.4 ms)

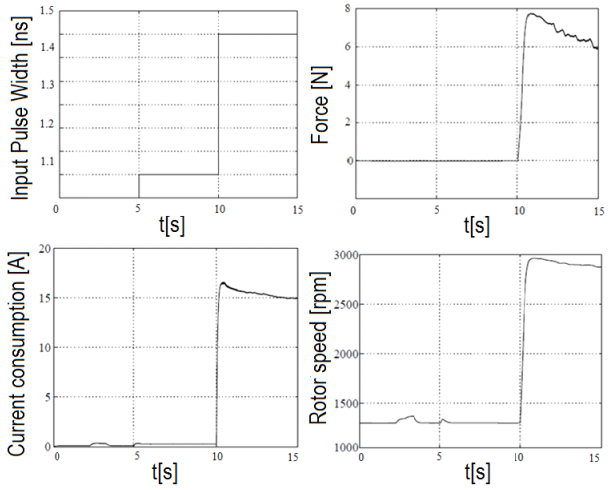

Fig. 9: Step response of the BLDC Thruster: high rotor speed regime (max pulse width 1.9 ms)

C. Example of a Simple Close Loop Controller

Finally, we illustrate the importance of a close loop controller on the performance of a thruster face to the aerodynamic load torque with a simple example. We implemented a PD compensator of the aerodynamic forces to regulate the rotor speed, and thus, the lift force. The step response of the system is showed in Figure 10 where we present a double step

experiment, first, in the low speed regime and then, in the high one. In both cases, overshot and steady state error are reduced, and the effects on the current consumption can be appreciated.

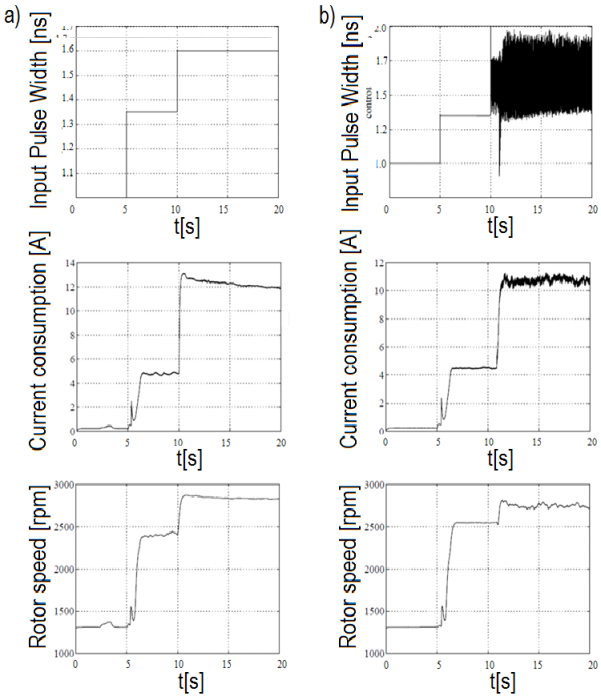

Fig. 10: BLDC Thruster dynamics: a) Open loop, b) Close loop by a PD speed controller

V. Conclusion

In this paper we analyzed and quantified the effects of the aerodynamic load torque on the performance of a BLDC thruster of small-scale quadrotors. We consider the dynamics of a BLDC thruster as the result of a hybrid system described as a composed model of a 3-phase BLDC motor and a two blade propeller of fixed pitch angle without twist, whose analytical expression, in terms of electric, mechanic and aerodynamic parameters, can be very useful for designing and control purposes, in particular for UAV applications. Numerical simulation of the BLDC/Propeller model showed the effects of the aerodynamic load torque on the ideal response of the thruster. The load torque, increasing non-linearly with respect to the angular speed of the propeller, enlarges the steady state error of the thruster response and reduces its bandwidth as the rotor is required to go faster. Experimental results realized on a standard aeromodelling BLDC thruster, validates the model in a low speed regime, showing a qualitatively similar response as that obtained by simulation; however, as the rotor speed is increased, aerodynamic forces modify the general dynamic of the system in such a way that overshoot, settling time, and steady state error, are far from the obtained numerically. This could be explained by the non-modelled dynamics of the air acting on the thruster (inertia and elasticity of the air stream), whose description requires further research of the aerodynamic phenomena in high speed regime and a better knowledge of the dynamic response of the commercial drivers. A better analytical description of the thruster dynamics is required to enable the use of modern control techniques to improve its response, and therefore, of the whole aircraft, either to assist operators in teleoperated flight or to assure stability in autonomous flight; including optimization criteria concerning its general performance considering its energy consumption. In order to illustrate the importance of designing close loop controllers to improve the dynamic response of the thrusters, we included some experimental results obtained with a PD compensator of the rotor speed.

Acknowledgment

Ricardo Martinez-Alvarado is supported by Conacyt Scholarship 233940. This work has been realized in the facilities of the Non Inertial Robotics and Man-Machine Interfaces Lab, CINVESTAV-Monterrey.

References

[1] G.M. Hoffmann, H.Huang, S.L. Waslander and C.J. Tomlin, *Quadrotor Helicopter Flight Dynamics and Control: Theory and Experiment*, Proceedings of the AIAA Guidance, Navigation and Control Conference, 2007.

[2] J.B. Brandt and M.S. Selig, *Propeller Performance Data at Low Reynolds Numbers*, Proceedings of the 49th AIAA Aerospace Sciences Meeting, 2011

[3] G. Sanahuja, *Commande et localisation embarque d'un drone aerien en utilisant la vision*, These Doctorale, Universite de Tecnologie de Compigne, France, 2010.

[4] Vinod K. R. Singh Patel, A. K. Pandey, *Modelling and Performance Analysis of PID Controlled BLDC Motor and Different Schemes of PWM Controlled BLDC Motor*, International Journal of Scientific and Research Publications, Vol. 3 Issue 4, 2013.

[5] P. Pounds, R. Mahony, P. Corke, *System Identification and Control of an Aerobot Drive System*, Information, Decision and Control Conference 2007, pp 154-159.

[6] R. Martinez-Alvarado, E. E. Granda-Gutierrez, A. E. Sanchez-Orta, A. E., F. J. Ruiz-Sanchez, *Modeling and Simulation of a System Propeller/Engine for Unmanned Aerial Vehicles*, Reunion of Power, Electronics and Computing IEEE ROPEC 2013, November 2013, Morelia, Mexico.

[7] J. Ren, H. Feng, H. Ren, and Y. Huang, *Simulation of PMSM Vector Control System Based on Propeller Load Characteristic*, International Conference on Intelligent Control and Information Processing, Dalian, China, 2010.

[8] D. Shang, Y. Liu, F. Sun, H. Zhang, *Study on DTC-SVM of PMSM Based on Propeller Load Characteristic*, Proceedings of the 7th World Congress on Intelligent Control and Automation, Chongqing, China, 2008.

[9] D. W. Novotny and T. A. Lipo, *Vector Control and Dynamics of AC Drives*, Oxford, Clarendon Press, p.213, 1996.

[10] R. Krishnan, *Electric Motor Drives: Modelling Analysis and Control*, New Jersey, Prentice Hall, pp. 577-614, 2001.

[11] J. Seddon, *Basic Helicopter Aerodynamics*, London, BSP Professional Books, pp. 5-8, 23-36, 1990.

[12] , B.W. McCormick, *Aeronautics and Flight Mechanics*, John Wiley and Sons, USA, 1995.

[13] J G. Leishman, *Principles of Helicopter Aerodynamics*, Cambridge University Press, USA, 2006.

[14] C.P. Singh, SS Kulkarni, S. C. Rana, Kapil Deo, *State-Space Based Simulink Modelling of BLDC Motor and its Speed Control using Fuzzy PID Controller*, International Journal of Advances in Engineering Science and Technology, V2 No3, pp 359-369, 2013.

[15] Maxon Precision Motors Inc, EC 45, 45 mm, Brushless, 150 Watt, CE approved, with Hall sensors. *http://www.maxonmotor.com/maxon/view/catalog/*, p. 16, 2012.